



João Pedro Rodrigues Branco de Almeida de Simões

Licenciado em Engenharia de Micro e Nanotecnologia

Development of paper transistor with memory effect

Dissertação para obtenção do Grau de Mestre em
Mestrado Integrado em Engenharia de Micro e Nanotecnologias - Engenharia de Micro e
Nanotecnologias

Orientador: Luís Miguel Nunes Pereira, Prof. Auxiliar, FCT-UNL

Júri:

Presidente: Doutor Rodrigo Ferrão de Paiva
Martins

Arguentes: Doutora Joana Maria Doria Vaz Pinto

Vogais: Doutor Luís Miguel Nunes Pereira



FACULDADE DE
CIÊNCIAS E TECNOLOGIA
UNIVERSIDADE NOVA DE LISBOA

Dezembro, 2015

Development of paper transistor with memory effect

Copyright © [João Pedro Rodrigues Branco de Almeida Simões], Faculdade de Ciências e Tecnologia, Universidade Nova de Lisboa. A Faculdade de Ciências e Tecnologia e a Universidade Nova de Lisboa têm o direito, perpétuo e sem limites geográficos, de arquivar e publicar esta dissertação através de exemplares impressos reproduzidos em papel ou de forma digital, ou por qualquer outro meio conhecido ou que venha a ser inventado, e de a divulgar através de repositórios científicos e de admitir a sua cópia e distribuição com objectivos educacionais ou de investigação, não comerciais, desde que seja dado crédito ao autor e editor.

Acknowledgments

Firstly, I would like to express my sincere gratitude to my supervisor Professor Luis Pereira and to Diana Gaspar for their continuous support and patience. Their guidance was of great help, particularly when it came to the laboratory work and interpretation of the results. I could not have imagined having a better advisors and mentors for my master's thesis.

I would like to thank the A3ple and FCT Funpaper projects for facilitating this line of research and thus giving this thesis wider appeal.

Thanks to the whole crew of CENIMAT and CEMOP | I3N and to the fellow master's student working under Professor Luis Pereira, for all their help and kindness in the day to day lab work and research.

Last but not the least, I would like to thank my family: my parents, my brother and sister and my friend Emanuel Miranda for supporting me and putting up with all the setbacks and complications throughout the completion of this work.

Resumo

Este trabalho discute o uso de três diferentes membranas de celulose nanofibrilada (NFC) como dielétrico para transístores de efeito de campo de memória. Duas das membranas receberam aditivos durante a fase de polpa, a uma foi adicionado Poliamidoamina-epicloridrina (PAE) e à outra HCl. A terceira membrana de referência não recebeu aditivos. Foi utilizado Óxido de Gálio Índio e Zinco (GIZO) como semicondutor do dispositivo e como eléctrodo de porta foi utilizado Óxido de Gálio Alumínio Zinco (GAZO). O conteúdo de água das membranas de papel foi determinado, antes e depois de vácuo, por espectroscopia de infravermelhos por transformada de Fourier (FTIR). Testes do desempenho eléctrico dos transístores revelaram uma razão I_{ON}/I_{OFF} máxima de cerca de $3,52 \times 10^5$ e um *subthreshold swing* de 0,804 V/década. O tempo de retenção da carga no dielétrico que concede ao transístor as suas capacidades de memória foi testado pela medição da corrente de dreno periodicamente durante 144 dias. Durante este período, a média da corrente de dreno não diminuiu, deixando o tempo de retenção do dispositivo indeterminado. Estes resultados foram comparados com dispositivos similares revelando que estes dispositivos estão dentro dos melhores no que toca ao estado da arte.

Palavras-chave: memória; transístor de papel; celulose; EDL; óxido de transístor de efeito de campo; RF pulverização catódica.

Abstract

This work will discuss the use of different paper membranes as both the substrate and dielectric for field-effect memory transistors. Three different nanofibrillated cellulose membranes (NFC) were used as the dielectric layer of the memory transistors (NFC), one with no additives, one with an added polymer PAE and one with added HCl. Gallium indium zinc oxide (GIZO) was used as the device's semiconductor and gallium aluminium zinc oxide (GAZO) was used as the gate electrode. Fourier transform infrared spectroscopy (FTIR) was used to access the water content of the paper membranes before and after vacuum. It was found that the devices recovered their water too quickly for a difference to be noticeable in FTIR. The transistor's electrical performance tests yielded a maximum ION/IOFF ratio of around $3,52 \times 10^5$ and a maximum subthreshold swing of 0,804 V/decade. The retention time of the dielectric charge that grants the transistor its memory capabilities was accessed by the measurement of the drain current periodically during 144 days. During this period the mean drain current did not lower, leaving the retention time of the device indeterminate. These results were compared with similar devices revealing these devices to be at the top tier of the state-of-the-art.

Keywords: Paper memory transistor; Cellulose; EDL; oxide field-effect transistor; RF magnetron sputtering

List of Abbreviations

ATR-FTIR - Attenuated total reflectance - Fourier transform infrared spectroscopy

BEKP - Bleached Eucalyptus Kraft Market Pulp

EDL - Electrical Double Layer

EEPROM - Electrically Erasable PROM

EPROM - Erasable PROM

FeFET – Ferroelectric FET

FET - Field-Effect Transistor

FT-IR - Fourier transform Infrared Spectroscopy

GAZO - Gallium–Aluminium-Zinc-Oxide

GIZO - Gallium–Indium–Zinc-Oxide

IZO - Indium–Zinc-Oxide

M-NFC - Microfibrillated/nanofibrillated Cellulose

NCC - Nanocrystalline Cellulose

NFC - Nanofibrillated Cellulose

PAE - Polyamidoamine-epichlorohydrin

PROM - Programmable ROM

RAM - Random-access memory

RH - Relative Humidity

ROM - Read-only memory

TFT –Thin-film transistor

List of symbols

C_i – Dielectric capacitance per unit area

Cl^- - Chlorine ion

F – Farad

f – Frequency

h – hour

H^+ - Hydrogen ion

HCl - Hydrochloric acid

Hz - Hertz

I_{DS} – Current between source and drain

I_G – Leakage current between gate and source

I_{OFF} – Drain current in the OFF state

I_{ON} – Drain current in the ON state

L – Channel length

m - metre

min – Minute

$^{\circ}C$ – Degrees Celsius

pH – Acidity or basicity of an aqueous solution

R^2 - Coefficient of determination

s - Second

V - Volt

V_{GS} – Voltage between gate and source

V_{ON} – Transistor ON voltage

V_{ON-1} – V_{ON} during the forward half of the hysteresis

V_{ON-2} – V_{ON} during the second half of the hysteresis

W – Channel width

μ_{sat} – Electron mobility in the saturation regime

List of Figures

Figure 2.1: Microscope images of the two possible alternatives for the devices' dimensions.....	15
Figure 3.1: Capacitance variation with frequency for the three paper membranes.....	18
Figure 3.2: Transfer characteristics of the transistors produced on the three types of paper: a) NFC-pure; b) NFC+PAE; c) NFC+ph 5.5.....	19
Figure 3.3: Transfer characteristics for the three transistors: a) NFC-pure; b) NFC+PAE; c) NFC+ph 5.5 at atmospheric pressure and after 10 minutes under vacuum.....	20
Figure 3.4: Transfer characteristics for the three transistors: a) NFC-pure; b) NFC+PAE; c) NFC+ph5.5 at atmospheric pressure (before vacuum) and during the first 10 min of recovery.....	21
Figure 3.5: Transfer characteristics for the three transistors: a) NFC-pure; b) NFC+PAE; c) NFC+ph5.5 at atmospheric pressure (before vacuum) and during recovery until no longer showing change (taking from 1h to 1h 30min to do it).....	22
Figure 3.6: Transfer characteristics of the NFC-pure transistor a) while undergoing vacuum; b) while recovering from vacuum at atmospheric pressure.....	23
Figure 3.7: Transfer characteristics of the NFC+PAE transistor a) while undergoing vacuum; b) while recovering from vacuum at atmospheric pressure.....	23
Figure 3.8: Transfer characteristics of the NFC+ph5.5 transistor a) while undergoing vacuum; b) while recovering from vacuum at atmospheric pressure.....	24
Figure 3.9: Example of a normalized ATR-FTIR spectrum of one of the NFCs.....	25
Figure 3.10: ATR-FTIR spectra of the NFC-pure sample normalized to the intensity of the band at 2900 cm^{-1} . Each graph shows the spectrum obtained before and after vacuum along with after 10 minutes of recuperation after vacuum. Figure 4.2 a) and b) correspond to 10 min of vacuum while c) and d) to 30 min of vacuum. Furthermore a) and c) are a zoom on the $3600\text{-}3000\text{ cm}^{-1}$ band while b) and d) are a zoom on the 1650 cm^{-1} band.....	26
Figure 3.11: ATR-FTIR spectra of the NFC+PAE sample normalized to the intensity of the band at 2900 cm^{-1} . Each graph shows the spectrum obtained before and after vacuum along with after 10 minutes of recuperation after vacuum. Figure 4.2 a) and b) correspond to 10 min of vacuum while c) and d) to 30 min of vacuum. Furthermore a) and c) are a zoom on the $3600\text{-}3000\text{ cm}^{-1}$ band while b) and d) are a zoom on the 1650 cm^{-1} band.....	27
Figure 3.12: ATR-FTIR spectra of the NFC+ph5.5 sample normalized to the intensity of the band at 2900 cm^{-1} . Each graph shows the spectrum obtained before and after vacuum along with after 10 minutes of recuperation after vacuum. Figure 4.2 a) and b) correspond to 10 min of vacuum while c) and d) to 30 min of vacuum. Furthermore a) and c) are a zoom on the $3600\text{-}3000\text{ cm}^{-1}$ band while b) and d) are a zoom on the 1650 cm^{-1} band.....	28
Figure 3.13: Obtained average I_D in open-gate configuration along with a logarithmic fit of I_D and the measured local RH for the three transistors: a) NFC-pure; b) NFC+PAE; c) NFC+ph5.5.....	29

List of Tables

Table 1.1: Types of semiconductor memories [13].....	12
Table 2.1: List of paper membranes used as dielectric for the paper FETs.....	14
Table 3.1: Lowest Pressure reached during vacuum according to the sample used and the duration of the vacuum.....	25
Table 3.2: Electrical performance of the obtained paper transistors.....	30
Table 3.3: Electrical performance of similar memory transistors.....	31

Table of Contents

1. INTRODUCTION.....	12
1.1 SEMICONDUCTOR MEMORIES.....	12
1.2 PAPER MEMORY TRANSISTOR.....	12
1.3 ELECTRICAL DOUBLE LAYER (EDL).....	13
1.4 COMPETING TECHNOLOGIES	14
2. MATERIALS AND METHODS.....	14
2.1 FABRICATION OF THE FETs.....	15
2.2 CHARACTERIZATION OF THE FETs AND PAPER MEMBRANES.....	15
3. RESULTS AND DISCUSSION	18
3.1 ELECTRICAL CHARACTERIZATION.....	18
3.2 VACUUM AND HUMIDITY	19
3.2.1 TRANSFER CHARACTERISTICS UNDER LOW VACUUM	19
3.2.2 TRANSFER CHARACTERISTICS UNDER HIGH VACUUM	23
3.2.3 ATR-FTIR MEASUREMENTS.....	25
3.3 CHARGE RETENTION TIME.....	29
3.4 SUMMARY OF RESULTS.....	30
3.5 COMPARISON WITH SIMILAR DEVICES.....	31

Motivation and Objectives

Motivation

Paper has received a recent growing interest in electronics research for a myriad of reasons including being cheap, flexible, recyclable, biocompatible and environmentally friendly [1]. Furthermore the technology for production and processing of paper has been improving for a long time; paper in roll-to-roll processing for example can reach up to $100\text{km}\cdot\text{h}^{-1}$ [1].

One of the simplest ways of using paper in electronics is as a substrate [2] [3] [4] [5]. But paper has also been used as an active component, mainly has a dielectric for capacitors [6] [7]. In 2008 Fortunato et al. reported for the first time the use of paper as the substrate and the dielectric layer of a thin-film field effect transistor (FET) [8]. This device showed a good electrical performance, with saturation mobility over $30\text{ cm}^2/\text{Vs}$ and an $I_{\text{ON}} / I_{\text{OFF}}$ ratio of around 10^4 ; along with a good stability and a low operating bias. It was later shown that since the paper membrane accumulates electric charges, the transistor's transfer characteristic gains a counterclockwise hysteresis. This accumulation can be taken advantage of in order to use these thin film transistors (TFT) as memory transistors [9]. This structure has been further investigated particularly by testing the influence of varying paper membranes on the influence of the devices [10] [11].

Continuing in this line of research, this work aims to test three nanofibrillated cellulose (NFC) membranes: a control membrane with no additives (NFC-pure); a membrane with an added wet-strength increasing polymeric resin (NFC+PAE) and a membrane whose original paper pulp was subjected to an addition of HCl (NFC+ph 5,5).

Objectives

The main goal for this work is to test the three previously mentioned membranes and the devices manufactured using them to uncover any differences in performance and to compare them to other memory transistors of similar architecture.

To this end, the transistors' electrical characteristics were measured not only in atmospheric pressure but in varying degrees of lower pressure in order to access the devices' dependence on the local relative humidity. Furthermore the water content of the membranes was also inferred through Fourier transform Infrared Spectroscopy (FT-IR), before and after being exposed to different degrees of vacuum.

Finally the performance of the devices as memories was analysed by assessing how long the devices can retain their state depending on paper polarization.

1. Introduction

1.1 Semiconductor memories

Within the context of computer memories, a distinction can be made between memories which can be directly accessed by a processing unit, and memories whose recording medium is not electronic in nature and thus requires a driver to convert information to electronic form [12]. The former memories are designated as electronic memories or more commonly as semiconductor memories due to being often made of inorganic semiconductors. These memories can also be categorised according to the criteria on Table 1.1.

Table 1.2: Types of semiconductor memories [13]

Memory type	Category	Erase	Write Mechanism	Volatility
Random-access memory (RAM)	Read-write memory	Electrically, bit-level	Electrically	Volatile
Read-only memory (ROM)	Read-only memory	Not possible	Masks	Nonvolatile
Programmable ROM (PROM)			Electrically	
Erasable PROM (EPROM)	UV light, chip-level			
Electrically Erasable PROM (EEPROM)	Electrically, bit-level			
Flash memory	Electrically, block-level			

1.2 Paper memory transistor

The proof of concept for the use of cellulose-fiber-based paper as both an active component and the substrate of thin-film field-effect transistors (FETs) was first presented in 2008 by Fortunato et al. [8]. In this previous work, as represented in Fig. 1.1, the paper was used as the thin-film transistor's (FET) dielectric; furthermore GIZO ($\text{Ga}_2\text{O}_3\text{-In}_2\text{O}_3\text{-ZnO}$; 1:2:1%mol) was used as the semiconductor channel, aluminium was used for the source and drain contacts, and IZO ($\text{In}_2\text{O}_3\text{-ZnO}$; 5:2 mol%) was used on the other side of the sheet as the gate contact.

In the same year, the same structure was used as a memory transistor [9]. This was made possible because the paper dielectric retains some polarization provided by the gate electrode (Fig. 1.2.). Furthermore, since the drain-to-source current (I_{DS}) only lowers back to the OFF-state by the use of a gate-to-source voltage

(V_{GS}), that is symmetric to the one used to set the device to the ON-state, the devices can be said to be selective, meaning they can each hold more than one bit of information [14].

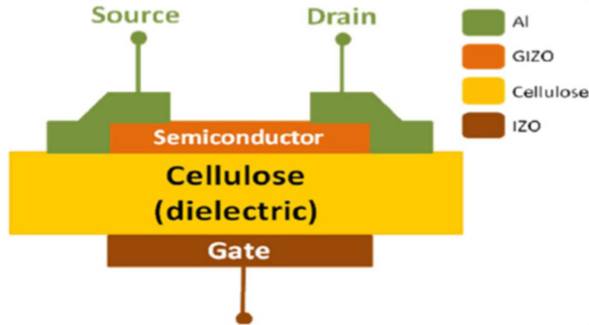


Figure 1.1: Schematic of the TFT's structure [8]

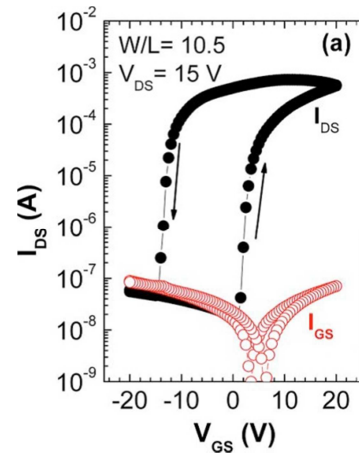


Figure 1.2: Transfer characteristic of a paper memory transistor [9]

Since these memories are erasable at the bit level, are non-volatile and since the data is written electrically; following Table 1.1, they could be classified as a form of Electrically Erasable Programmable Read-only memory (EEPROMs). Later in 2014, it was found that adding HCl to the cellulose pulp leads to an increase in the performance of the transistor, measurable through both the saturation mobility and the I_{ON}/I_{OFF} ratio [15].

1.3 Electrical Double Layer (EDL)

In 2014, nanocrystalline cellulose (NCC) and microfibrillated/nanofibrillated cellulose (M-NFC) paper membrane were measured in order to access the capacitance's response to the applied frequency [10], [15]. It was found that the obtained response greatly resembles the data from electric double-layer (EDL) capacitors [16] and electrolyte-gated FETs [17], particularly when it comes to the increase of the membranes capacitance at low frequency values. This has led to the conclusion that the paper membranes also form EDL when used as dielectrics [10], [15].

The EDL consists of two parallel planes. The first compact layer adsorbed to the electrode made up of dipole or charged molecules oriented or complementing the electrode's charge. The second layer is attracted to the first via the coulomb force; this second layer less strongly attached and thus more diffuse [18], [19]. They may be composed of dipole molecules, monoatomic or polyatomic ions. EDLs form, amongst other ways, on the interfacial region between charged electrodes and electrolytes [18], [19].

The EDL has an associated capacitance, and this is believed to be the main variable when it comes to the paper's dielectric performance, particularly for low frequencies [10], [15]. Furthermore due to the thinness and locality of the EDL, not only will the dielectrics capacitance be relatively high, it will also be independent of the dielectrics actual thickness [17].

Finally, it was found that relative humidity RH, also had an effect on the performance of EDL dielectrics, both in the case of paper [15] and other EDL based dielectrics [16], [17]. Multiple reasons are given for this; for one

the presence of the dipolar water molecules will lead to the break of molecules held by ionic bonds; this will lead to an increase of charges within the dielectric and thus an increase in capacitance [16]. Also, the presence of the water molecules increases the mobility of the charges as well, particularly by allowing free protons to be transferred between water molecules through hydrogen bonds [17].

1.4 Competing technologies

The two main alternative forms of storing information in the dielectric layer are the trapping of charges throughout the dielectric, or the polarization of ferroelectric dielectrics [20]. There are of course other similar devices with multiple layers, but those will not be addressed in this work.

In the case of electrets, the electric field may be maintained through the presence of accumulated charges or through the polarization of electric dipoles through the dipoles [21]. Thus, the electret memories function similarly to an EDL, though their performance will be more dependent on the thickness of the dielectric. Nonetheless, the electric field contained in dielectric will eventually dissipate either by losing accumulated charge through leakage current or due to the reorientation of the dipoles back into a random state after de-removal of the external electric field. Hence it is said that the electrets are merely meta-stable [21].

Ferroelectrics however, due to being in thermodynamic equilibrium, will maintain their state virtually forever [22]. Some of the main challenges that ferroelectric field-effect transistors (FeFET) face are the lack of thermal stability of the interface with the semiconductor and the trapping of electric charges at the same interface. To counter these issues, buffer layers have been used between the semiconductor and ferroelectric to protect the semiconductor from the high-temperature annealing procedures used for inorganic ferroelectrics and to prevent charge injection from the semiconductor to the ferroelectric [23]. Also, it is predicted that FeFET scaling will be limited to 22 nm since the properties of the ferroelectrics with respect to thickness dependence of the electrical field will not allow further reduction [24].

2. Materials and methods

In order to study the influence that different cellulosic membranes have on the memory's performance, a set of three different nanofibrillated cellulose membranes (NFC) were used as the dielectric layer of the memory transistors (Tab. 2.1). One NFC had no additives, a polymer Polyamidoamine-epichlorohydrin (PAE) was added to the second type whereas HCl was added to the third type. PAE is a polymeric resin used to increase the wet-strength of paper, as in the mechanical resistance of paper to sheer pressure when wet. This is achieved by the way PAE bonds different paper fibres and thus maintains their structure when they swell due to moisture absorbance [25]. The three membranes were obtained from an outside source, manufactured according to table 2.1

Table 2.1: List of paper membranes used as dielectric for the paper FETs.

Sample	Kind of pulp	Additives
NFC-pure	BEKP [Bleached Eucalyptus Kraft Market Pulp]	None
NFC+PAE	BEKP	PAE resin
NFC+ph 5,5	NFC-Hardwood, enzymatic pre-treatment, GEA homogenizer	HCl

2.1 Fabrication of the FETs

For the fabrication of the FETs the semiconductor used was GIZO ($\text{Ga}_2\text{O}_3\text{-In}_2\text{O}_3\text{-ZnO}$; 1:2:1%mol) which was deposited at room temperature by radio frequency magnetron sputtering using an AJA ORION system. The gallium aluminium zinc oxide (GAZO) gate electrode was also deposited via sputtering. Finally the aluminium source and drain electrodes were deposited using e-beam evaporation. This final aluminium deposition was also used to metalize the paper membranes in order to measure their capacitance later. After the depositions the transistors were annealed on a heating plate at 150°C in atmospheric pressure.

The FETs' structure was the same as the one used by Fortunato et al. [8] Figure 1.1 but using GAZO instead of IZO as the gate electrode.

Two W/L ratios were used for the devices, 6.6 and 10.6. The dimensions of the devices can be seen in the top view images Figure 1.2.

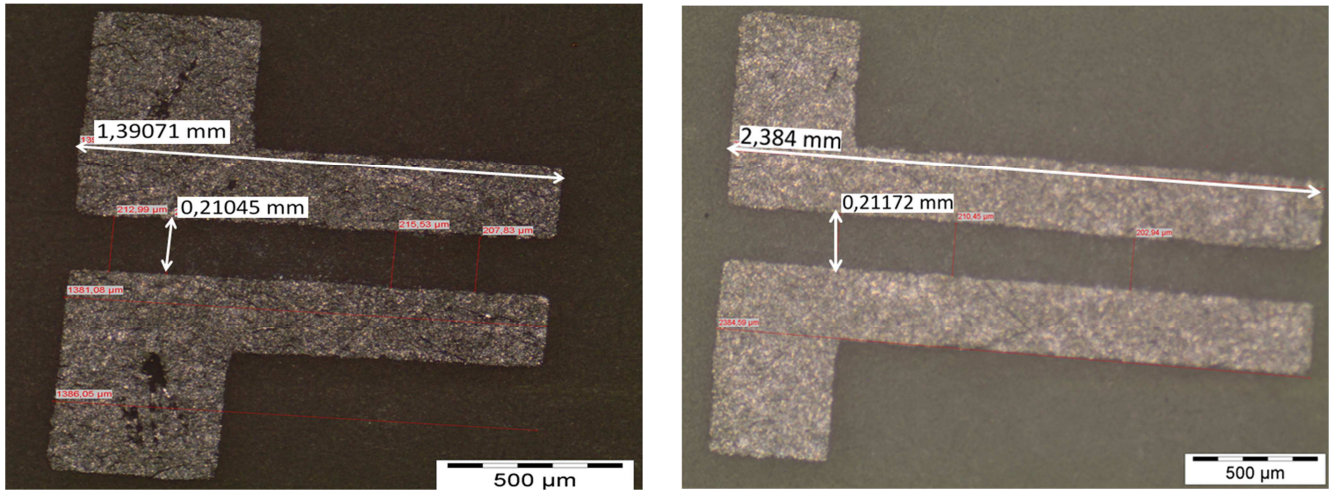


Figure 2.1: Microscope images of the two possible alternatives for the devices' dimensions

2.2 Characterization of the FETs and paper membranes

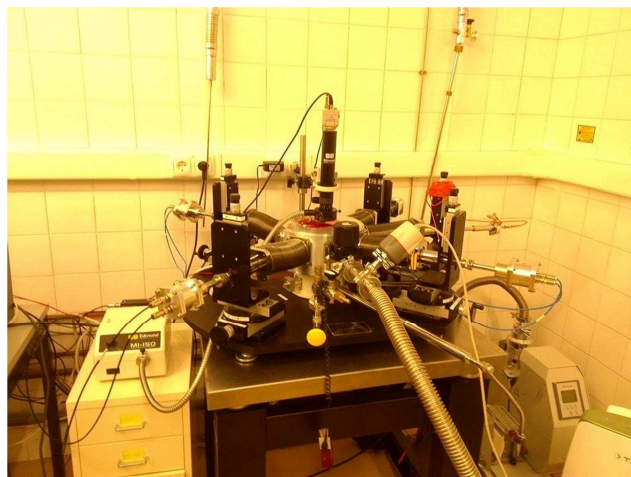
The membrane's electrical capacitance was measured through impedance spectroscopy using a Gamry Instruments Reference 600 Potentiostat in a parallel plate configuration.

The device's electrical performance was measured in ambient pressure using an Agilent 4155C semiconductor parameter analyser along with a Cascade Microtech M150 microprobe station using the Metrics ICS software. While in vacuum, a Keithley 4200-SCS semiconductor characterization system with a Cryogenic Equipment by JANIS Probe Station. Gate tensions used varied from -15V to 10V and the Drain voltage was 10V .

The saturation mobility of the devices was calculated through the following equation [26].

$$\mu_{\text{sat}} = \frac{\left(\frac{\partial \sqrt{I_D}}{\partial V_G}\right)^2}{\frac{1}{2} C_i \frac{W}{L}} \quad (2.1)$$

In order to confirm and reaccess the relationship between these devices and the local relative humidity (RH), the transistors were submitted to low vacuum (using a KNF NEUBERGER Type: N 035.3 AN.18) and to high vacuum (using an Edwards EXT 75DX 24V Turbo Molecular High Vacuum Pump) along with a hygrometer (RS #2410WC). The devices were left under vacuum for around 10 minutes until the pressure inside the vacuum chamber stabilized. After vacuum, the devices were left to recover from their loss of water by being exposed to atmospheric pressure.



a)

b)

Figure 2.2: Images of the Agilent 4155C semiconductor parameter analyser a); and the Keithley 4200-SCS semiconductor characterization system b).

FTIR measurements were performed to the paper membranes (simple paper without transistors) before and after submitting the paper membranes to vacuum using a Thermo Nicolet 6700 FT-IR Spectrometer.



Figure 2.3: Image of the Thermo Nicolet 6700 FT-IR Spectrometer

In order to determine how long the devices could retain their memory, they were each charged by measuring the forward half of their transfer characteristics. Posteriorly the drain current (I_D) was measured during 1 minute in an open gate configuration. These measurements were done various times during 144 days. The local temperature and relative humidity (RH) were also measured each time I_D was evaluated.

3. Results and Discussion

3.1 Electrical characterization

The impedance spectroscopy measurements led to the data in Figure 3.1. As was mentioned before, these results correspond to an EDL like dielectric as expected for these paper membranes [10] [11].

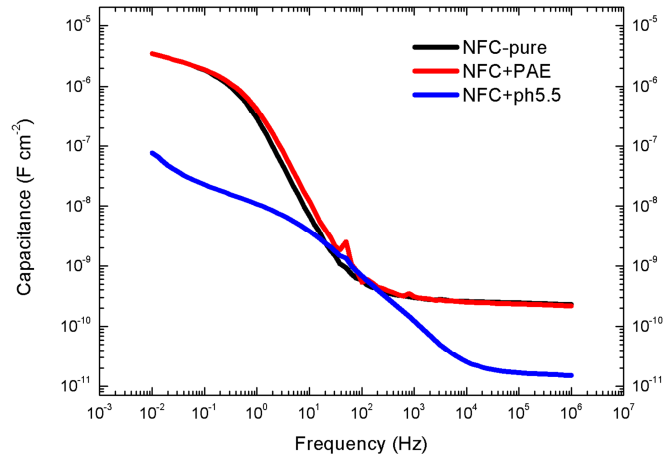


Figure 3.1: Capacitance variation with frequency for the three paper membranes.

The device's electrical characterization for transistors produced on the three membranes yielded the transfer characteristics represented on Figure 3.2. The device's electrical characterization showed a counterclockwise hysteresis, along with having a depletion n-type operation (Figure 3.2). The rest of the device's electrical properties such as the saturation mobility and the hysteresis associated turn-on voltage shift will be discussed at the end of this section.

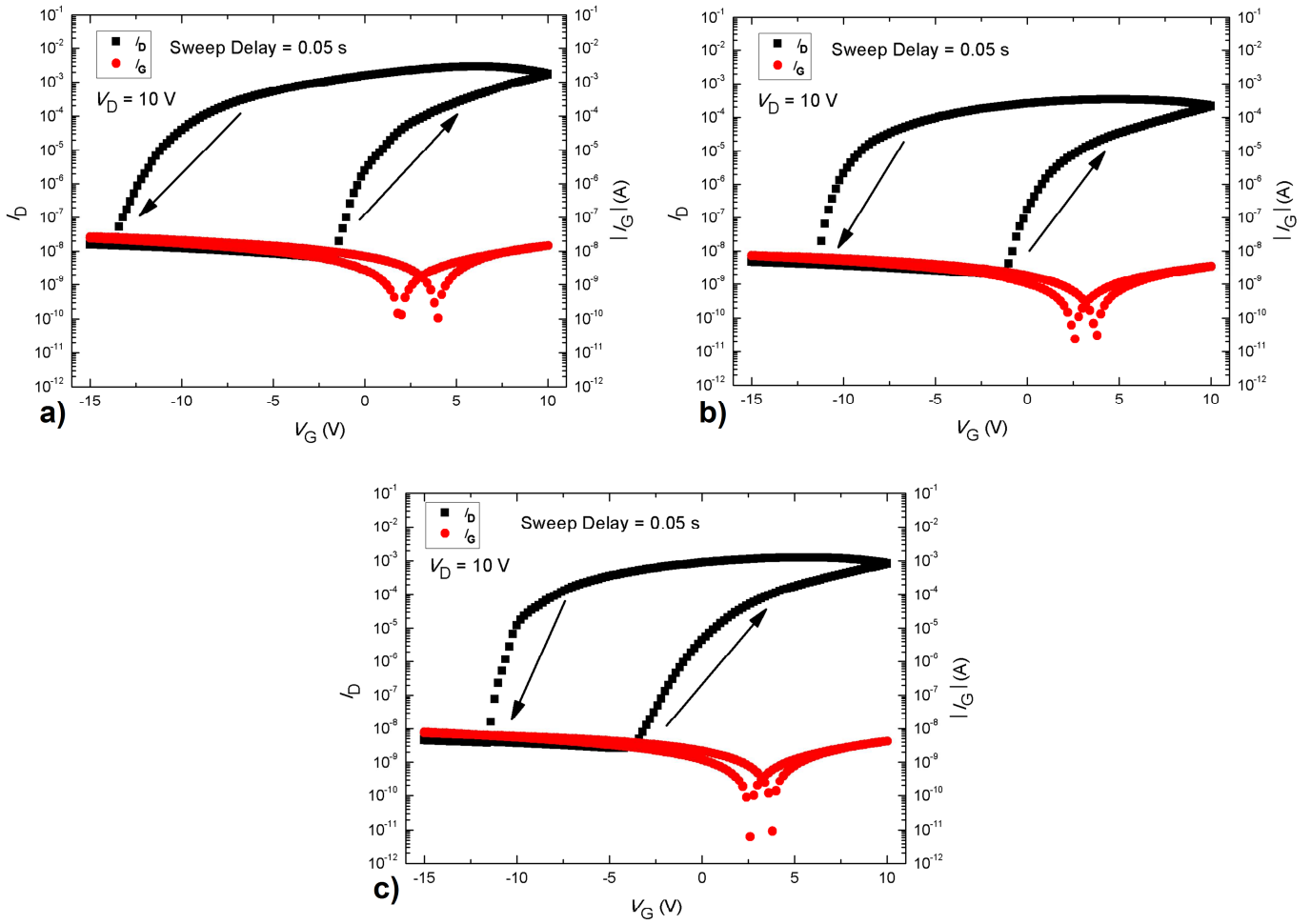


Figure 3.2: Transfer characteristics of the transistors produced on the three types of paper: a) NFC-pure; b) NFC+PAE; c) NFC+ph 5.5

3.2 Vacuum and Humidity

3.2.1 Transfer characteristics under low vacuum

Although the influence of vacuum on the transfer characteristics of paper transistor has already been studied [15], there hasn't been a study of how the turn-on voltage shift is affected by it. Thus this has been evaluated by this work.

When analysing the relationship between the three devices and the local relative humidity (RH), by submitting the transistors to low vacuum along with a hygrometer, we observed that, a mere 10% variation in relative humidity (RH), already leads to variations in the transfer curves (Figure 3.2.). Namely, a decrease in RH lead to an increase in the hysteresis associated turn-on voltage shift along with a decrease in both the I_{ON} and I_{OFF} ; the overall I_{ON} / I_{OFF} ratio decreased as well.

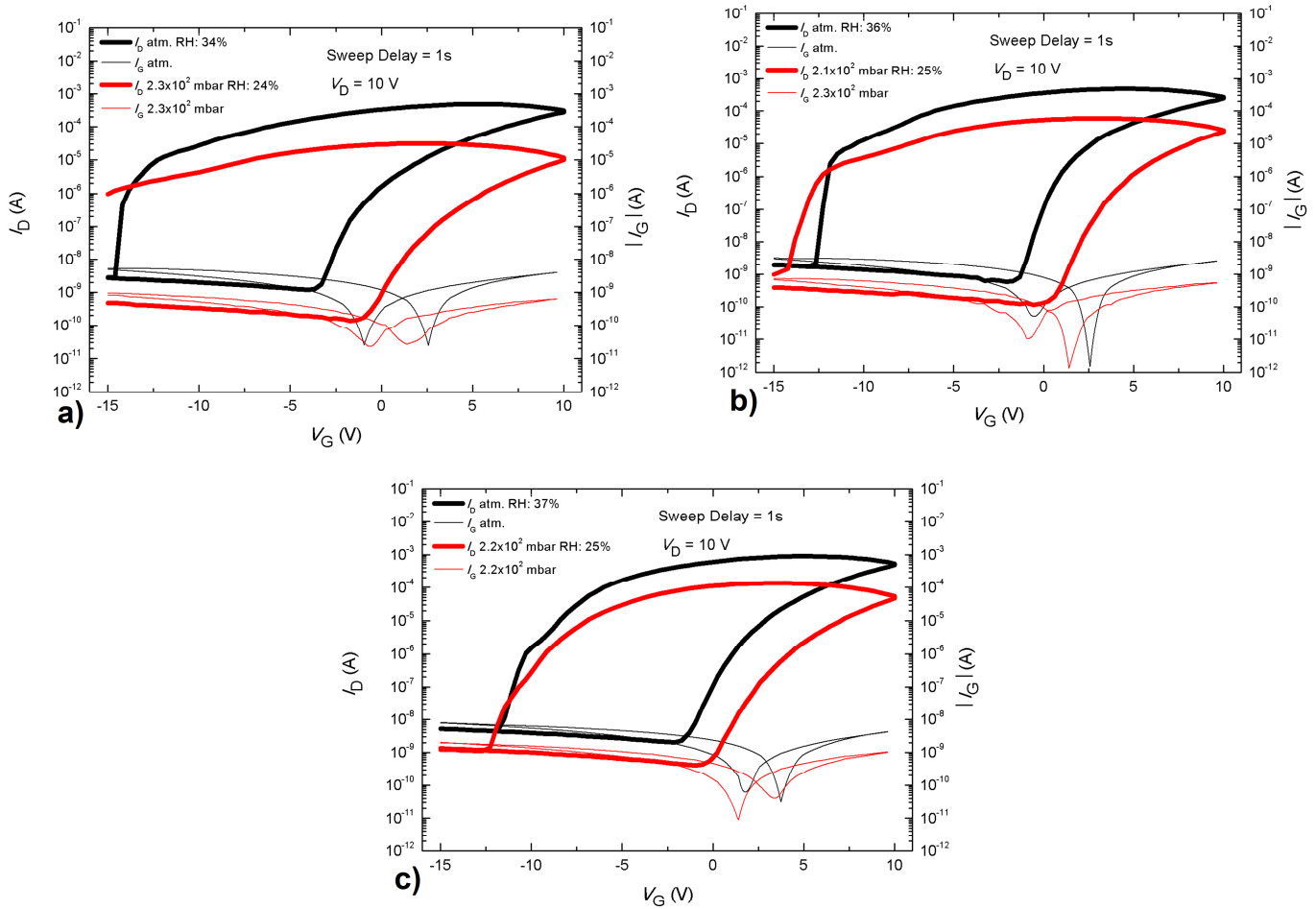
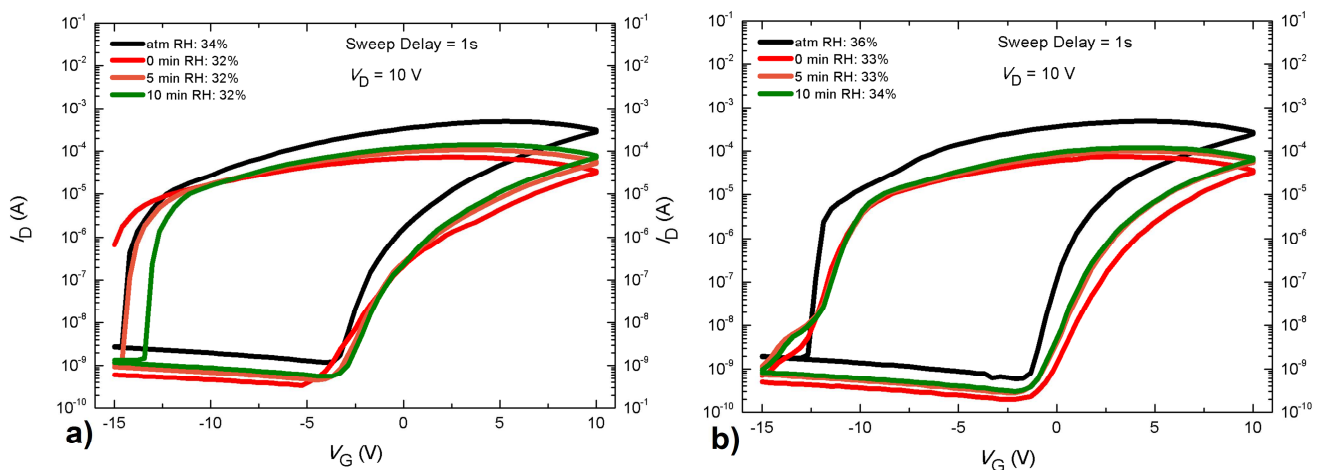


Figure 3.3: Transfer characteristics for the three transistors: a) NFC-pure; b) NFC+PAE; c) NFC+ph 5.5 at atmospheric pressure and after 10 minutes under vacuum

These changes are ultimately due to a change in RH. As mentioned before, water molecules not only increase the capacitance of the paper dielectric but also improve the whole device's electrical performance [15], mainly by increasing the I_{ON} / I_{OFF} ratio. Whether this happens due to an increase in mobile charges, an increase in mobility of already present charges or a mixture of both has not yet been uncovered. However this distinction is not strictly necessary for an understanding of these changes in performance.



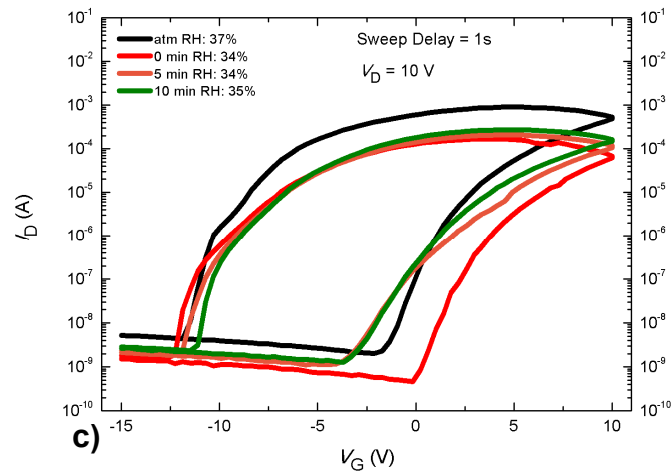


Figure 3.4: Transfer characteristics for the three transistors: a) NFC-pure; b) NFC+PAE; c) NFC+ph5.5 at atmospheric pressure (before vacuum) and during the first 10 min of recovery

Regardless of why it happens, as the water content diminishes, so does the ability of the dielectric to produce charge accumulation in the channel layer. This can be seen for example in the increase of V_{ON} during the forward half of the hysteresis (V_{ON-1}), which then leads to an increase of the hysteresis associated V_{ON} shift.

Furthermore, I_{ON} lowers along with the I_{ON} / I_{OFF} ratio. We can also observe a decrease in $|I_G|$ due to the dielectric's reduced conductance. Since I_{OFF} is limited by I_G , the decrease of the latter will lower the former as well.

Finally, during low vacuum, one can observe a decrease of V_{ON} during the second half of the hysteresis (V_{ON-2}) in both Figure 3.3 a) and b). In fact the devices don't completely turn off within the voltage range used. This further contributes to an increase in hysteresis. Whereas other changes due to vacuum may be attributed to both or either a decrease in the total amount of charge within the dielectric or a decrease in their mobility of, in this particularly case the difference should be due to a decrease in mobility alone. This is inferred from the mechanism which provides the devices their hysteresis in the first place, the charge trapping in the dielectric.

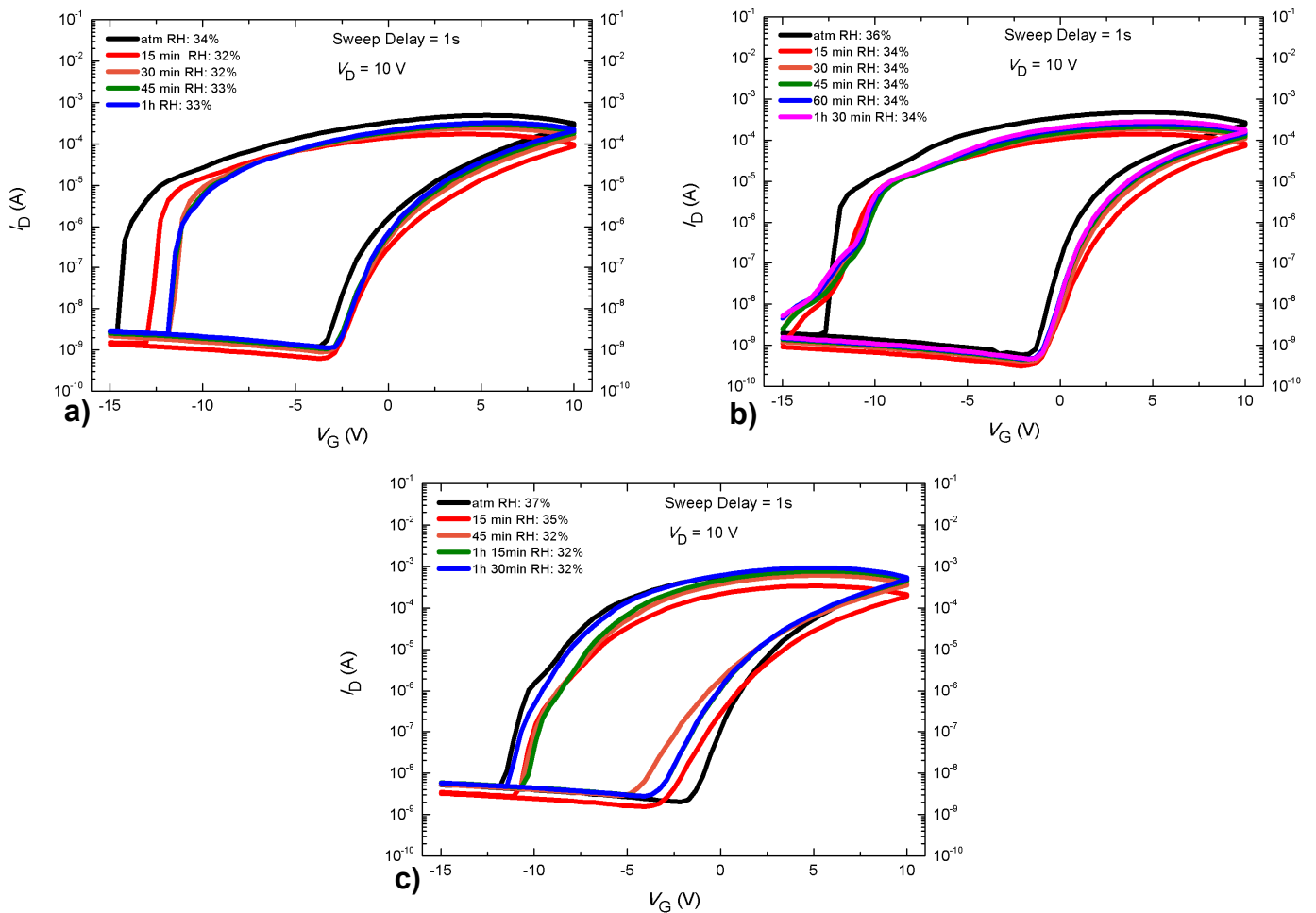


Figure 3.5: Transfer characteristics for the three transistors: a) NFC-pure; b) NFC+PAE; c) NFC+ph5.5 at atmospheric pressure (before vacuum) and during recovery until no longer showing change (taking from 1h to 1h 30min to do it).

The loss of the total amount of charge can only account for a decrease in its concentration at the EDL region. This observed decrease in V_{ON-2} however is due to an increase of the energy necessary to remove the charges left near the semiconductor during the first half of the hysteresis cycle, and thus is only related to a loss of mobility of them.

Nonetheless this loss of mobility, if measured by the decrease of V_{ON-2} , can be seen to be less noticeable in NFC+PAE and virtually inexistent in NFC+ph 5.5 (Figure 3.3). For the latter it is understandable that the increase in concentration of the highly mobile H^+ ions stemming from the added HCl would counteract any loss of mobility of charges. As for the NFC+PAE, since PAE is a cationic polymer [27], its presence may help the movement of mobile charges. Furthermore (PAE) may also hinder the loss of water in the first place; this later point will be expanded upon on section 3.2.3.

We can finally see that NFC+PAE and NFC+ph 5.5 are also more resistant to a decrease of I_{ON} , I_{OFF} and I_{ON}/I_{OFF} ratio. This may very well be for the same reasons given above for V_{ON-2} , with the added fact that NFC+ph 5.5 has greater amount of charges due to the exposure to HCl.

The transfer characteristics measured throughout the first 10 minutes of recovery process after vacuum can be seen in Figure 3.4. Through it, one can see that all of the previously mentioned features recover somewhat within this 10 min; though only the two V_{ON} (both V_{ON-1} and V_{ON-2}) make a total recovery.

In fact, it took an hour and a half for the devices to make a good recovery, and even then, neither NFC-pure nor NFC+PAE fully recovered the original I_{ON} values (Figure 3.5.). It is also of note that NFC-pure seems to be the most sensible when it comes to V_{ON-2} . It actually increased beyond the value before vacuum.

3.2.2 Transfer characteristics under high vacuum

To understand how the devices behave when RH is even lower, they were submitted to a higher vacuum until completely losing their ability to modulate I_D (Figures 3.6, 3.7 and 3.8).

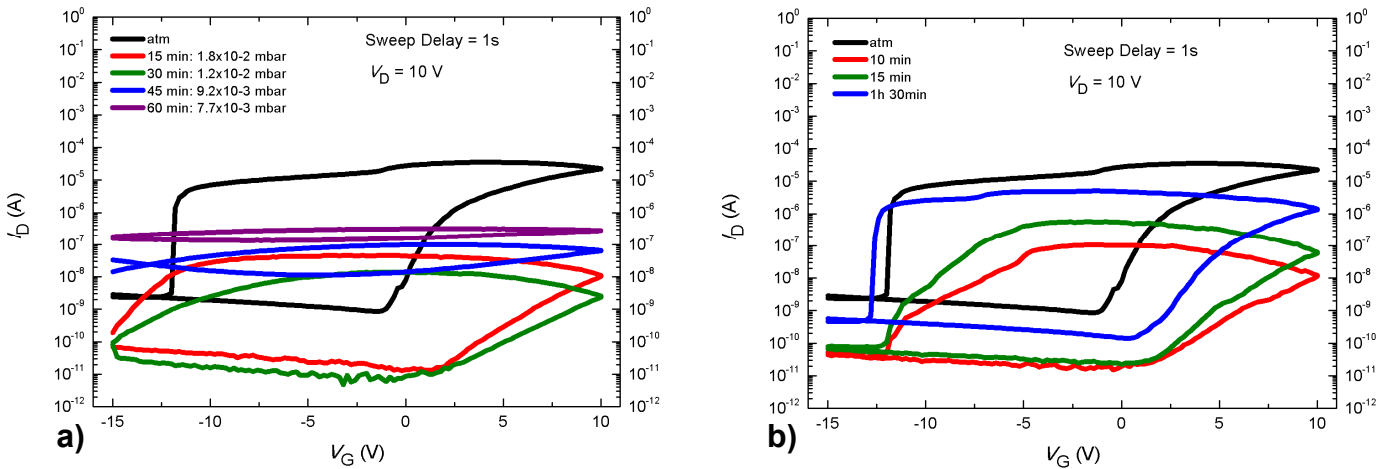


Figure 3.6: Transfer characteristics of the NFC-pure transistor a) while undergoing vacuum; b) while recovering from vacuum at atmospheric pressure.

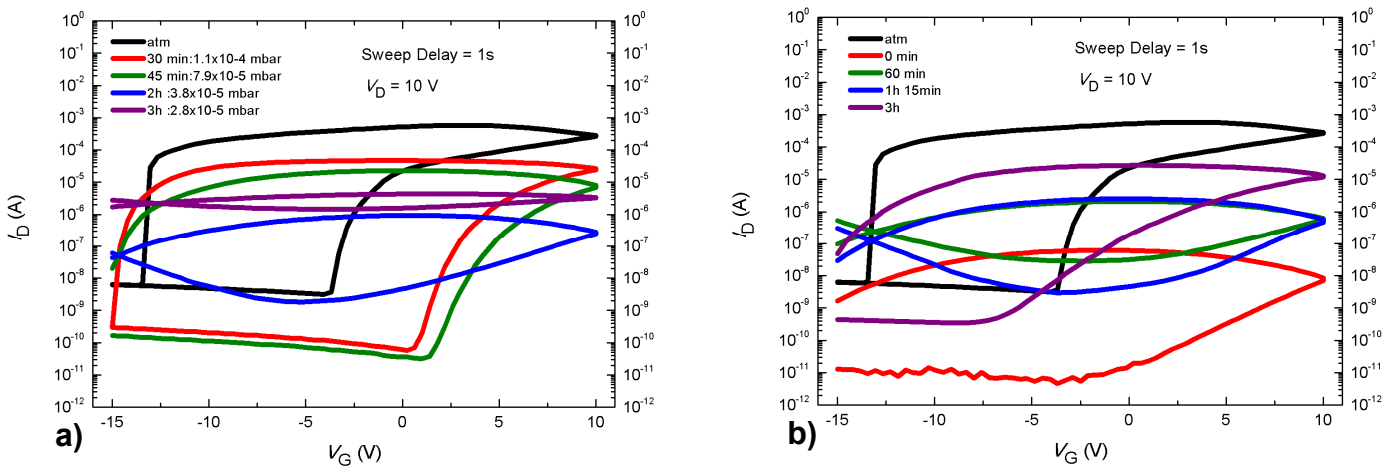


Figure 3.7: Transfer characteristics of the NFC+PAE transistor a) while undergoing vacuum; b) while recovering from vacuum at atmospheric pressure.

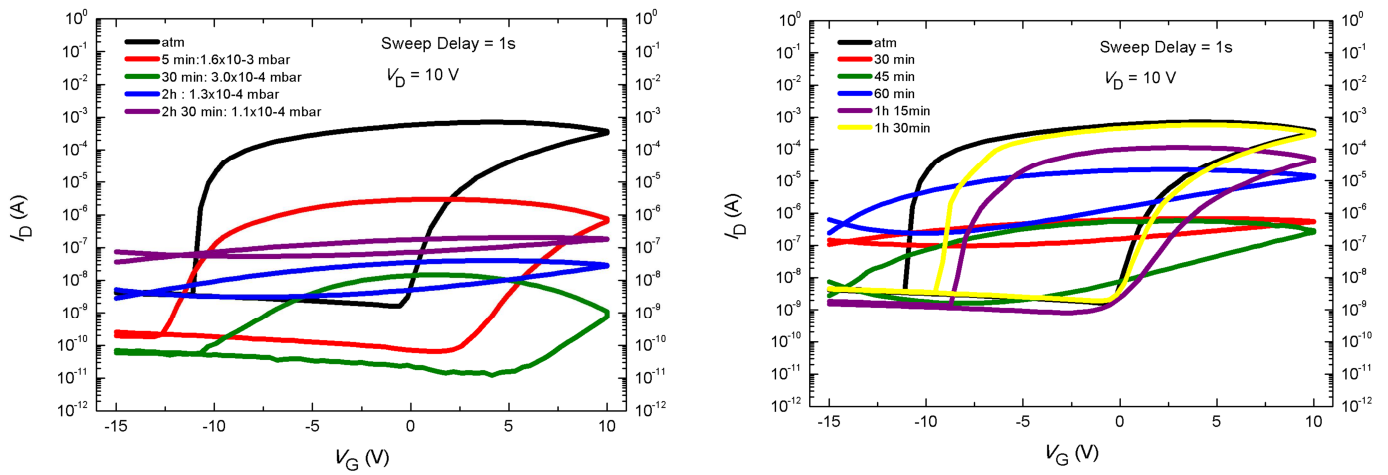


Figure 3.8: Transfer characteristics of the NFC+ph5.5 transistor a) while undergoing vacuum; b) while recovering from vacuum at atmospheric pressure.

An interesting thing to note is the way I_{ON} and I_{OFF} change throughout the vacuum process. Initially, like mentioned before, both I_{ON} and I_{OFF} decrease, but as $|V_G|$ reaches a minimum and as the ability of the dielectric to modulate I_D decreases both I_{ON} and I_{OFF} shift toward the current value corresponding to the unmodulated GIZO.

Just like during low vacuum, the amount of time the devices were left under vacuum is not enough for them to recover to their original performance. However in this case, NFC+ph5.5 is an exception since it recovers its original I_{ON} / I_{OFF} ratio in a shorter time than the time it spent under vacuum. Since NFC+ph5.5 has the added H^+ charges it is less dependent on water to maintain its performance. As soon there is enough water to allow adequate charge mobility, the device recovers its performance. Furthermore these added charges also increase the resilience of the device to the exposure to vacuum, being able to last 2h and 30min, more than twice of NFC-pure (Figure 3.6 and 3.7).

On the other hand the addition of PAE seems to increase both the time it takes for the device to lose its capacity for modulation and the time it takes to recover said capacity Figure 3.7. Due to the results presented in the next section (3.2.3), the reason for this difference seems to come from the way this polymer affects the loss and reabsorption of water by the paper membrane.

3.2.3 ATR-FTIR measurements

FTIR measurements were taken before and after submitting the paper membranes to vacuum, to assess the relative water content. The pressures reached during vacuum are indicated in Table 3.1.

Table 3.1: Lowest Pressure reached during vacuum according to the sample used and the duration of the vacuum

Sample	10 min	30 min
NFC-pure	1.9×10^{-2} mbar	1.3×10^{-2} mbar
NFC+PAE	2.1×10^{-2} mbar	1.0×10^{-2} mbar
NFC+ph 5.5	2.0×10^{-2} mbar	8.9×10^{-3} mbar

The relative water content can be qualitatively determined by comparing the intensity of the absorbance bands between $3600\text{-}3000\text{ cm}^{-1}$ and at 1650 cm^{-1} [28]. The first band is associated to the asymmetric and symmetric stretching of water molecules strongly bonded to the cellulose's and hemicelluloses' OH groups via hydrogen bonding and to water molecules weakly bonded to the same groups via another water molecule [28]. The second is associated to the H-O-H angle vibration and thus to free water molecules [28].

At 2900 cm^{-1} lies the absorption band corresponding to the stretching of C-H groups. This band is insensitivity not only to the cellulose's water content, but also to variations in composition and crystallinity [29]. Therefore, in the present work the FTIR spectra were normalized according to the peak of 2900 cm^{-1} (Figure 3.8.)

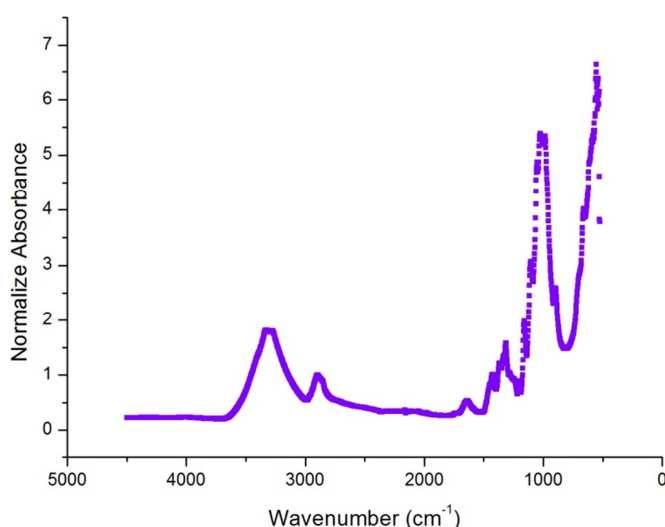


Figure 3.9: Example of a normalized ATR-FTIR spectrum of one of the NFCs

In order to more closely observe the differences between spectra, the previously mentioned bands were zoomed in, leading to Figure 3.10, 3.11 and 3.12.

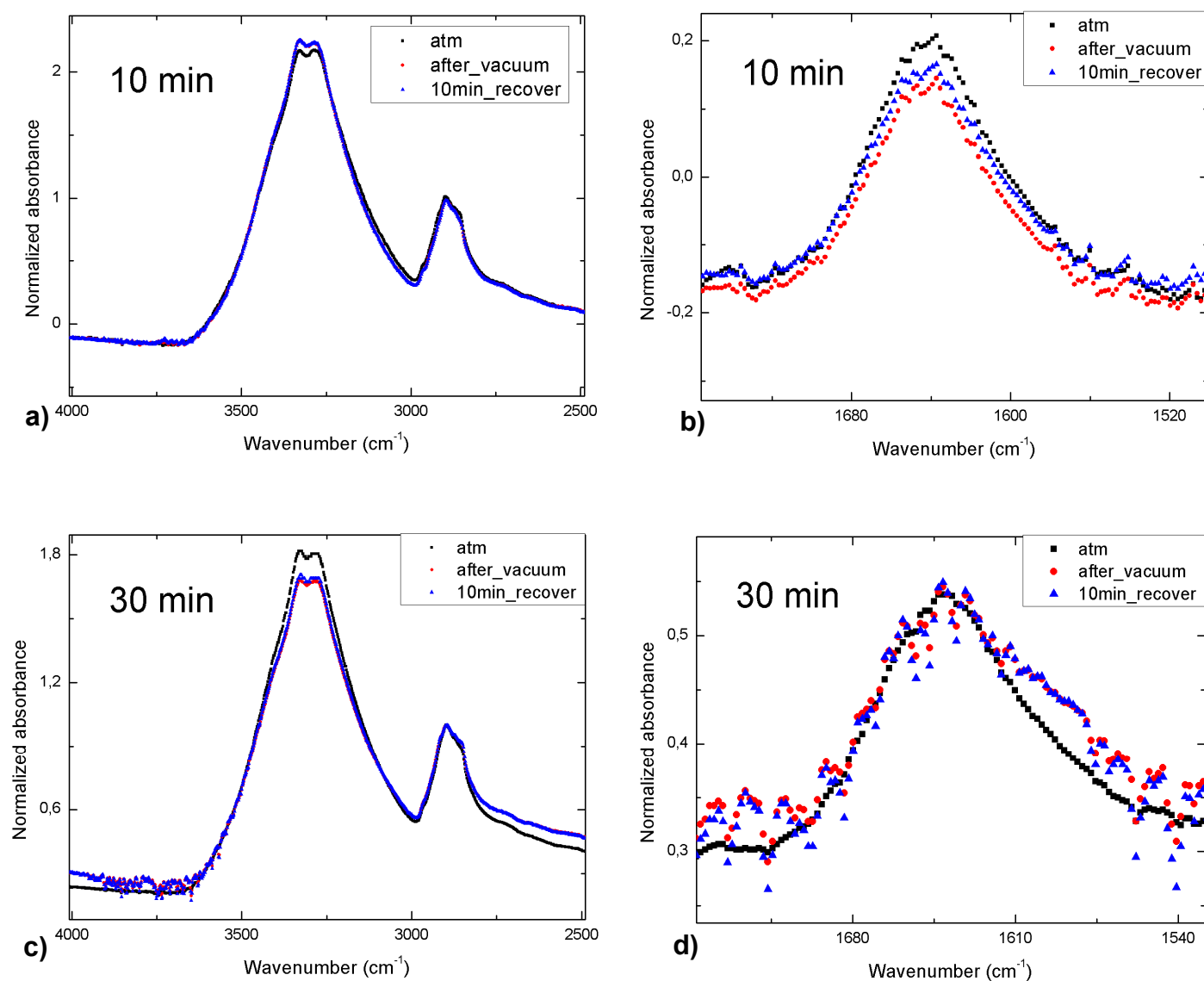


Figure 3.10: ATR-FTIR spectra of the NFC-pure sample normalized to the intensity of the band at 2900 cm^{-1} . Each graph shows the spectrum obtained before and after vacuum along with after 10 minutes of recuperation after vacuum. Figure 4.2 a) and b) correspond to 10 min of vacuum while c) and d) to 30 min of vacuum. Furthermore a) and c) are a zoom on the 3600-3000 cm^{-1} band while b) and d) are a zoom on the 1650 cm^{-1} band

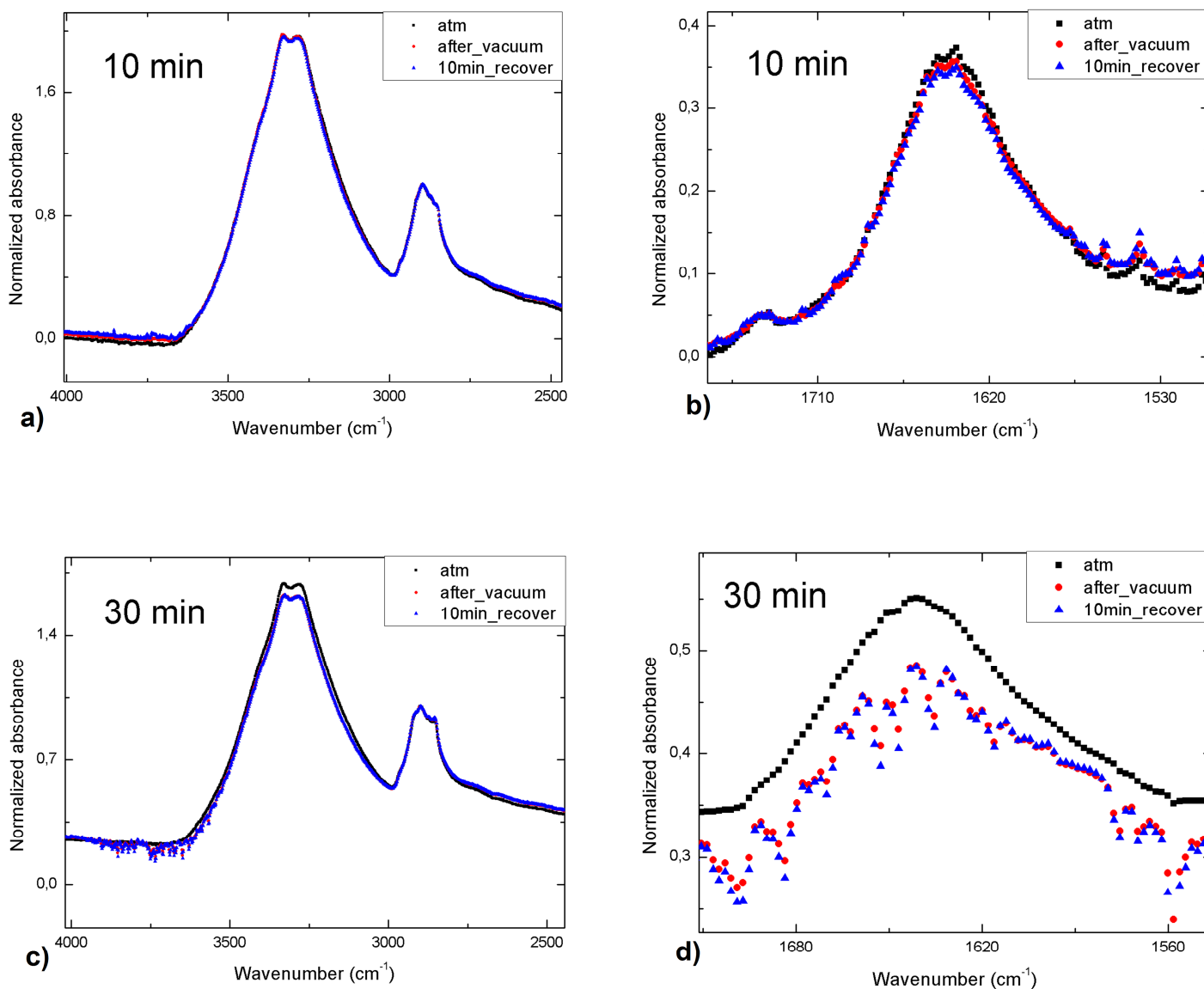


Figure 3.11: ATR-FTIR spectra of the NFC+PAE sample normalized to the intensity of the band at 2900 cm^{-1} . Each graph shows the spectrum obtained before and after vacuum along with after 10 minutes of recuperation after vacuum. Figure 4.2 a) and b) correspond to 10 min of vacuum while c) and d) to 30 min of vacuum. Furthermore a) and c) are a zoom on the $3600\text{--}3000\text{ cm}^{-1}$ band while b) and d) are a zoom on the 1650 cm^{-1} band

As the 'after_vacuum' and '10min_recover' lines seem to always coincide, 10 minutes appear to make practically no difference when it comes to the membranes' water content.

Also this data seems to corroborate what was previously mentioned concerning the way PAE increases the ability of the paper membranes to resist the loss of performance through exposure to vacuum. In Figure 3.11 a) and b) there is visibly no difference between the obtained pre and post-vacuum spectra. This shows that the 10 minutes of vacuum were not sufficient to achieve a low enough pressure capable of removing water from the NFC+PAE membrane.

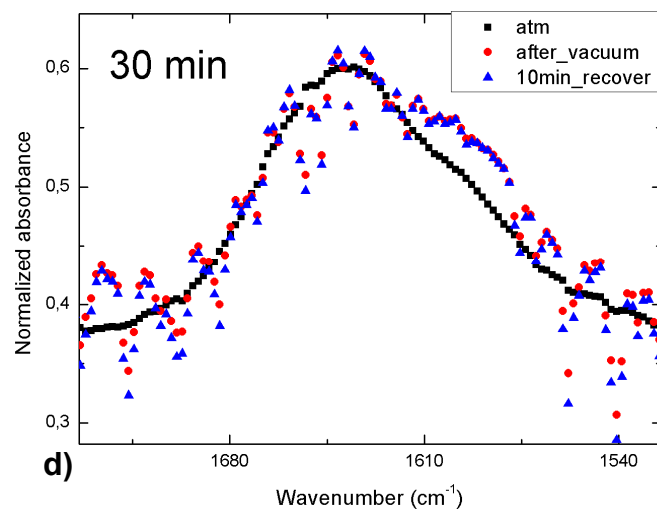
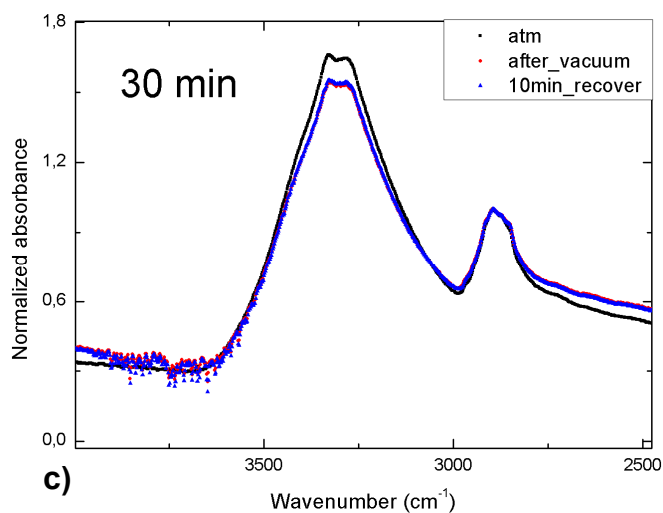
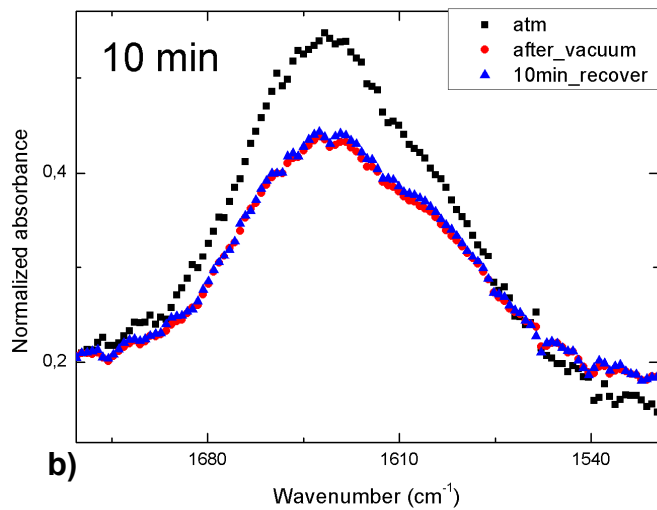
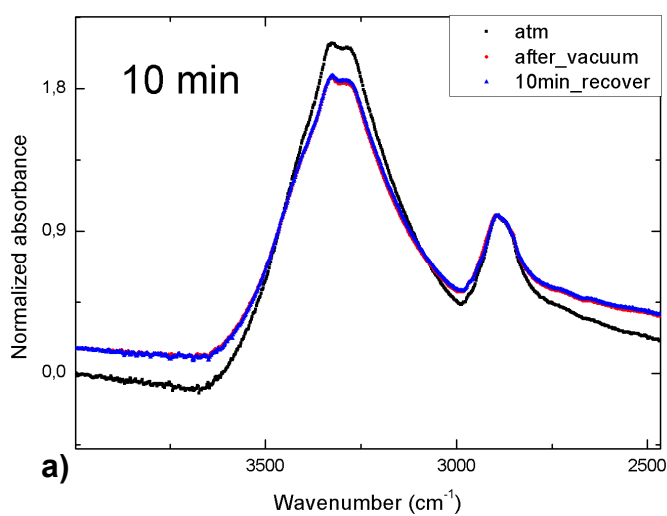


Figure 3.12: ATR-FTIR spectra of the NFC+ph5.5 sample normalized to the intensity of the band at 2900 cm^{-1} . Each graph shows the spectrum obtained before and after vacuum along with after 10 minutes of recuperation after vacuum. Figure 4.2 a) and b) correspond to 10 min of vacuum while c) and d) to 30 min of vacuum. Furthermore a) and c) are a zoom on the $3600\text{-}3000 \text{ cm}^{-1}$ band while b) and d) are a zoom on the 1650 cm^{-1} band

Since NFC+ph5.5 (Figure 3.12) and NFC-pure (Figure 3.10) don't differ much in their spectra, we can confirm that the added resilience of NFC+ph5.5's performance to vacuum is due to the charges added by the HCl exposure and not due to a different affinity to water.

Something to note is that at Figure 3.10 a), it seems that the amount of water in the membrane actually increased after vacuum, this may be due to an actual increase of RH in the ambient room between measurements.

Another point is that even though differences in the baselines were overall corrected for comparison between spectra, this was not done for Figure 3.12 a). This is because even without aligning the baseline it is already observable that there is a decrease in the water content, aligning the baselines would only increase the difference between the spectra. The problem is that aligning the baseline would disrupt the normalization to the 2900 cm^{-1} band.

3.3 Charge retention time

The measurement of I_D for the three devices during 141 days led to the data on Figure 3.13.

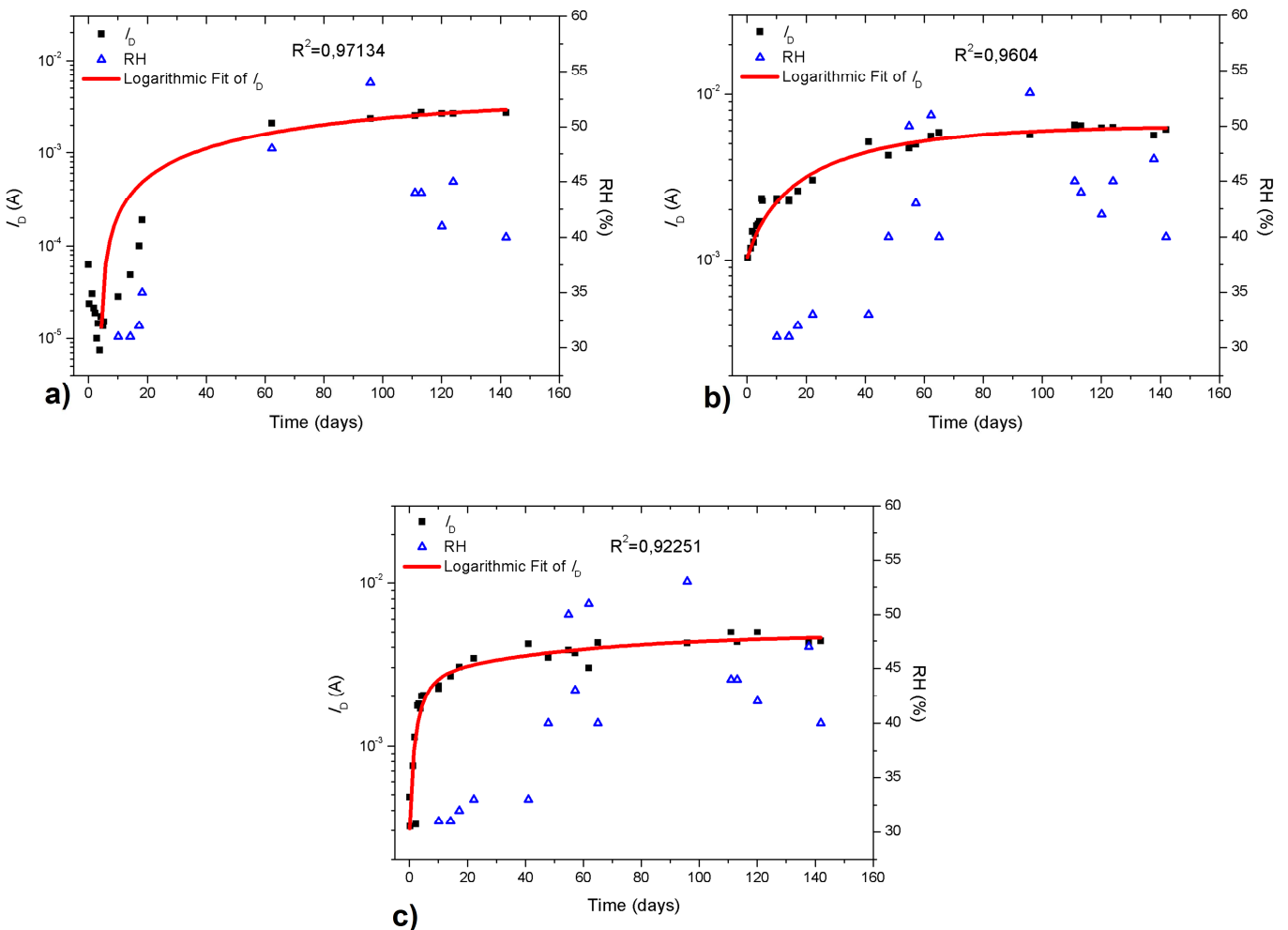


Figure 3.13: Obtained average I_D in open-gate configuration along with a logarithmic fit of I_D and the measured local RH for the three transistors: a) NFC-pure; b) NFC+PAE; c) NFC+ph5.5

A logarithmic function was fitted to the data leading to values of R^2 over 0.92 Figure 3.13. As can be seen in Figure 3.13, there is an initial increase in I_D until it saturates. Since no gate voltage is applied it seems that the act of measuring I_D actually increases it, thus helping maintaining the charge. This could also be due to an increase of the overall humidity but there is low correlation with it after the current stabilizes Figure 3.13. The obtained temperature values also did not show much correlation with I_D .

Given that I_D shows no sign of decreasing, it is impossible to extrapolate how long the devices can store there memory.

Table 3.2: Electrical performance of the obtained paper transistors

Dielectric	I_{ON} / I_{OFF} ratio	Maximum voltage (V)	Tested retention time (days)	Extrapolated retention time	Capacitance per unit area ($F.cm^{-2}$)	Saturation Mobility ($cm^2.V^{-1}.s^{-1}$)	V_{ON} shift (V)	Subthreshold swing (V/decade)	Maximum Temperature
NFC-pure	3.52×10^5	15	144	Indeterminate	3.46×10^{-6}	5.56	12.2	0.474	150°C
NFC+PAE	1.08×10^5	15	144	Indeterminate	3.45×10^{-6}	0.482	10.6	0.587	150°C
NFC+ph5.5	1.28×10^5	15	144	Indeterminate	7.64×10^{-8}	55.6	8.2	0.804	150°C

3.4 Summary of results

The summary of the results obtained for the three transistors, taking the charge retention time data along with the previous results into account, are presented in Table 3.2. The saturation mobility was calculated according to the (2.1) equation in section 2.2. The capacitance registered is the one obtained from the impedance spectroscopy measurements (Figure 3.1)

It is of note that the devices' performances are essentially the same with the exception of NFC+ph5.5. The dielectric's capacitance per unit area is two orders of magnitude smaller than the rest. This may be due to the Cl^- ions left from the HCl treatment, due to these ions' low mobility; they may remain in the EDL formation zone despite being repelled by the local electric field. This will disturb the device's ability to accumulate charges in the form of the EDL and thus reduce the membranes capacitance.

Despite this, the device's I_{ON} / I_{OFF} ratio remains close to the rest. It is hypothesized that this is due to the greater concentration in H^+ which may migrate into the GIZO and thus increase its mobility, hence the high saturation mobility of this transistor. This phenomenon has already been demonstrated at least for ZnO [30],

3.5 Comparison with similar devices

The data of similar memory transistors, divided by the type of dielectric, meaning either electrets or ferroelectrics was compiled from previous literature (Table 3.3). Added to these results are the maximum voltage used during the electric performance tests and the maximum temperature used during the manufacture of the devices. This comparison permits the study of the low-cost potential and portability of future devices based on these transistors. The transistor's electrical performance tests all yielded a I_{ON}/I_{OFF} ratio of around 10^5 , including the one found in present work, with the exception of Faber et al. (2009) [31] which showed a higher performance. This is also the only article which presents the subthreshold swing of the devices.

When it comes to the present work, the retention time is possibly surpassed only by Naber et al. (2005b) [36]. Although not the lowest, the electric voltages used were among the lowest (Tables 3.3) the temperatures were however in the average range.

Table 3.3 Electrical performance of similar memory transistors

Reference	I_{ON} / I_{OFF} ratio	Maximum voltage (V)	Retention time test	Extrapolated retention time	Subthreshold swing (V/decade)	Maximum Temperature (°C)
Electrets						
Gherendi et al. (2013) [32]	6×10^4	5V	>several days	--	0.3-0.5	--
Faber et al. (2009) [31]	10^6	25V	--	--	--	100 °C
Singh et al. (2004) [33]	10^4	80V	>15h	--	--	--
Singh et al. (2005) [34]	--	60 V	--	--	--	250 °C
Cai et al. (2007) [35]	10^3	100 V	70 min	--	--	70 °C

Ferroelectrics						
Reference	I_{ON} / I_{OFF} ratio	Maximum voltage (V)	Retention time test	Extrapolated retention time	Subthreshold swing (V/decade)	Maximum Temperature (°C)
Tripathi et al. (2011) [37]	10^5	40V	>10000s ~2,7 h	--	--	--
Naber et al. (2005a) [23]	10^3	100 V	1 week	--	--	138 °C
Schroeder et al. (2004a) [38]	200	20 V	Lost 20% of I_D after 3h	--	--	--
Schroeder et al. (2004b) [39]	2.7×10^4	40 V	>14h	--	--	50°C
Unni et al. (2004) [40]	--	40 V	Lost 20% of I_D after 5h	--	--	145°C
Naber et al. (2005b) [36]	--	20 V	1 week	>10 years	--	138°C
Gelinck et al. (2005) [41]	5×10^3	15 V	Lost 20% of I_D after 3h	--	--	140°C
Nguyen et al. (2006) [42]	--	120 V	--	--	--	140°C

4. Conclusions

As expected the obtained devices show a depletion n-type operation and a counterclockwise hysteresis. The transistor's electrical performance tests all yielded a I_{ON}/I_{OFF} ratio of around 10^5 .

The devices showed a variation in performance with as little as a 10% variation of relative humidity (RH). The addition of Polyamidoamine-epichlorohydrin (PAE) made it harder to remove water from the paper membrane but it also increased the time the membrane takes to recover the water content. On the other hand the addition of HCl to the paper pulp led a greater resilience to the effects of vacuum, not so much because of a difference of affinity to water, but due to the high mobility H^+ charges added by the HCl exposure.

I_D was measured in open gate configuration for 144 days showing no sign of decreasing, leaving the full charge retention time indeterminate. However it is expected that this time should be quite high for the three devices since the highest extrapolated time on similar devices was >10 years from Naber et al.(2005b) [36] which verified a decrease in I_D in as little as 7 days.

When it comes to energy expenditure, although not the lowest, the electric voltages used were among the lowest. The temperatures were however in the average range.

5. Future Perspectives

Due to the charge retention tests being inconclusive, further and longer tests could be made in order to establish a limit to how long the charges could be maintained. Furthermore a passivation of the devices after submitting them to a high humidity environment could prove to increase their electrical performance. Another way the dependence of the performance on humidity could be tested is by determining the influence of different levels of hydrophilicity of paper membranes on the devices' transfer characteristics.

In order to further decrease the voltage used one could consider lowering V_D even if this means using the device in linear mode.

Finally to further decrease the production costs, other methods of production, particularly ones compatible with the current printing technology should be tested such as ink-jet or even reel-to-reel processing.

6. References

- [1] D. Tobjörk and R. Österbacka, "Paper Electronics," *Adv. Mater.*, vol. 23, no. 17, pp. 1935–1961, 2011.
- [2] A. Manekkathodi, M.-Y. Lu, C. W. Wang, and L.-J. Chen, "Direct Growth of Aligned Zinc Oxide Nanorods on Paper Substrates for Low-Cost Flexible Electronics," *Adv. Mater.*, vol. 22, no. 36, pp. 4059–4063, 2010.
- [3] D.-H. Kim, Y.-S. Kim, J. Wu, Z. Liu, J. Song, H.-S. Kim, Y. Y. Huang, K.-C. Hwang, and J. A. Rogers, "Ultrathin Silicon Circuits With Strain-Isolation Layers and Mesh Layouts for High-Performance Electronics on Fabric, Vinyl, Leather, and Paper," *Adv. Mater.*, vol. 21, no. 36, pp. 3703–3707, 2009.
- [4] M. Hilder, B. Winther-Jensen, and N. B. Clark, "Paper-based, printed zinc–air battery," *J. Power Sources*, vol. 194, no. 2, pp. 1135–1141, 2009.
- [5] Y.-H. Kim, D.-G. Moon, and J.-I. Han, "Organic TFT array on a paper substrate," *Electron Device Lett. IEEE*, vol. 25, no. 10, pp. 702–704, 2004.
- [6] Y. Tanaka, N. Ishii, J. Okuma, and R. Hara, "Electric double-layer capacitor having a separator made from a cellulose fiber." Google Patents, 1999.
- [7] V. L. Pushparaj, M. M. Shaijumon, A. Kumar, S. Murugesan, L. Ci, R. Vajtai, R. J. Linhardt, O. Nalamasu, and P. M. Ajayan, "Flexible energy storage devices based on nanocomposite paper," *Proc. Natl. Acad. Sci.*, vol. 104, no. 34, pp. 13574–13577, 2007.
- [8] E. Fortunato, N. Correia, P. Barquinha, L. Pereira, G. Goncalves, and R. Martins, "High-performance flexible hybrid field-effect transistors based on cellulose fiber paper," *IEEE Electron Device Lett.*, vol. 29, no. 9, pp. 988–990, 2008.
- [9] R. Martins, P. Barquinha, L. Pereira, N. Correia, G. Gonçalves, I. Ferreira, and E. Fortunato, "Write-erase and read paper memory transistor," *Appl. Phys. Lett.*, vol. 93, no. 20, p. 203501, 2008.
- [10] D. Gaspar, S. N. Fernandes, A. G. de Oliveira, J. G. Fernandes, P. Grey, R. V Pontes, L. Pereira, R. Martins, M. H. Godinho, and E. Fortunato, "Nanocrystalline cellulose applied simultaneously as the gate dielectric and the substrate in flexible field effect transistors.," *Nanotechnology*, vol. 25, no. 9, p. 094008, 2014.
- [11] L. Pereira, D. Gaspar, D. Guerin, a Delattre, E. Fortunato, and R. Martins, "The influence of fibril composition and dimension on the performance of paper gated oxide transistors.," *Nanotechnology*, vol. 25, p. 094007, 2014.
- [12] A. K. Sharma, *Advanced Semiconductor Memories: Architectures, Designs, and Applications*. Wiley-IEEE Press, 2009.
- [13] W. Stallings, *Computer organization and architecture : designing for performance*. Boston: Pearson, 2013.
- [14] R. Martins, P. Barquinha, L. Pereira, N. Correia, G. Gonçalves, I. Ferreira, and E. Fortunato, "Selective floating gate non-volatile paper memory transistor," *Phys. Status Solidi - Rapid Res. Lett.*, vol. 3, no. 9, pp. 308–310, 2009.
- [15] L. Pereira, D. Gaspar, D. Guerin, A. Delattre, E. Fortunato, R. Martins, N. Correia, and P. Barquinha, "The influence of fibril composition and dimension on the performance of paper gated oxide transistors.," *Nanotechnology*, vol. 25, no. 9, p. 094007, 2014.
- [16] L. Ma and Y. Yang, "Solid-state supercapacitors for electronic device applications," *Appl. Phys. Lett.*,

vol. 87, no. 12, p. -, 2005.

- [17] O. Larsson, E. Said, M. Berggren, and X. Crispin, "Insulator Polarization Mechanisms in Polyelectrolyte-Gated Organic Field-Effect Transistors," *Adv. Funct. Mater.*, vol. 19, no. 20, pp. 3334–3341, 2009.
- [18] J. Heinze, "Electrochemistry, Principles, Methods, and Applications. Von C. M. A. Brett und A. M. O. Brett. Oxford University Press, Oxford, 1993. 427 S., Broschur 25.00 £. – ISBN 0-19-855388-9," *Angew. Chemie*, vol. 106, no. 22, pp. 2441–2442, 1994.
- [19] R. Parsons, "The electrical double layer: recent experimental and theoretical developments," *Chem. Rev.*, vol. 90, no. 5, pp. 813–826, 1990.
- [20] H. E. Katz, X. M. Hong, A. Dodabalapur, and R. Sarpeshkar, "Organic field-effect transistors with polarizable gate insulators," *J. Appl. Phys.*, vol. 91, no. 3, pp. 1572–1576, 2002.
- [21] G. M. Sessler, J. van Turnhout, B. Gross, M. G. Broadhurst, G. T. Davis, S. Mascarenhas, J. E. West, and R. Gerhard(-Mulhaupt), "Electrets, 2nd enlarged edition," *Top. Appl. Phys.*, vol. 33, p. XV+457–pages, 1987.
- [22] O. Auciello, J. F. Scott, and R. Ramesh, "The Physics of Ferroelectric Memories," *Print Ed.*, vol. 51, no. 7, 1998.
- [23] R. C. G. Naber, C. Tanase, P. W. M. Blom, G. H. Gelinck, A. W. Marsman, F. J. Touwslager, S. Setayesh, and D. M. de Leeuw, "High-performance solution-processed polymer ferroelectric field-effect transistors," *Nat Mater*, vol. 4, no. 3, pp. 243–248, Mar. 2005.
- [24] H. Kohlstedt, Y. Mustafa, A. Gerber, A. Petraru, M. Fitsilis, R. Meyer, U. Böttger, and R. Waser, "Current Status and Challenges of Ferroelectric Memory Devices," *Microelectron. Eng.*, vol. 80, pp. 296–304, 2005.
- [25] T. Obokata, M. Yanagisawa, and A. Isogai, "Characterization of polyamideamine-epichlorohydrin (PAE) resin: Roles of azetidinium groups and molecular mass of PAE in wet strength development of paper prepared with PAE," *J. Appl. Polym. Sci.*, vol. 97, no. 6, pp. 2249–2255, 2005.
- [26] D. Gupta, D. Gupta, M. Katiyar, and D. Gupta, "Mobility estimation incorporating the effects of contact resistance and gate voltage dependent mobility in top contact organic thin film transistors," *Indian Inst. Technol. Kanpur*, pp. 425–428, 2006.
- [27] T. Obokata and A. Isogai, "The mechanism of wet-strength development of cellulose sheets prepared with polyamideamine-epichlorohydrin (PAE) resin," *Colloids Surfaces A Physicochem. Eng. Asp.*, vol. 302, no. 1–3, pp. 525–531, 2007.
- [28] A.-M. Olsson and L. Salmén, "The association of water to cellulose and hemicellulose in paper examined by FTIR spectroscopy," *Carbohydr. Res.*, vol. 339, no. 4, pp. 813–818, 2004.
- [29] J. Łojewska, P. Miśkowiec, T. Łojewski, and L. M. Proniewicz, "Cellulose oxidative and hydrolytic degradation: In situ FTIR approach," *Polym. Degrad. Stab.*, vol. 88, no. 3, pp. 512–520, 2005.
- [30] H. Yuan, H. Shimotani, A. Tsukazaki, A. Ohtomo, M. Kawasaki, and Y. Iwasa, "Hydrogenation-Induced Surface Polarity Recognition and Proton Memory Behavior at Protic-Ionic-Liquid/Oxide Electric-Double-Layer Interfaces," *J. Am. Chem. Soc.*, vol. 132, no. 19, pp. 6672–6678, 2010.
- [31] H. Faber, M. Burkhardt, A. Jedaa, D. Kälblein, H. Klauk, and M. Halik, "Low-Temperature Solution-Processed Memory Transistors Based on Zinc Oxide Nanoparticles," *Adv. Mater.*, vol. 21, no. 30, pp. 3099–3104, 2009.

- [32] F. Gherendi, M. Nistor, and N. B. Mandache, "In₂O₃ Thin Film Paper Transistors," *Disp. Technol. J.*, vol. 9, no. 9, pp. 760–763, 2013.
- [33] T. B. Singh, N. Marjanović, G. J. Matt, N. S. Sariciftci, R. Schwödiauer, and S. Bauer, "Nonvolatile organic field-effect transistor memory element with a polymeric gate electret," *Appl. Phys. Lett.*, vol. 85, no. 22, pp. 5409–5411, 2004.
- [34] T. B. Singh, N. Marjanović, P. Stadler, M. Auinger, G. J. Matt, S. Günes, N. S. Sariciftci, R. Schwödiauer, and S. Bauer, "Fabrication and characterization of solution-processed methanofullerene-based organic field-effect transistors," *J. Appl. Phys.*, vol. 97, no. 8, p. 083714, 2005.
- [35] C. Xiuyu, C. P. Gerlach, and C. D. Frisbie, "Current-voltage hysteresis and memory effects in ambipolar organic thin film transistors based on a substituted oligothiophene," *J. Phys. Chem. C*, vol. 111, no. 1, pp. 452–456, 2007.
- [36] R. C. G. Naber, B. de Boer, P. W. M. Blom, and D. M. de Leeuw, "Low-voltage polymer field-effect transistors for nonvolatile memories," *Appl. Phys. Lett.*, vol. 87, no. 20, p. art. – 203509, 2005.
- [37] A. K. Tripathi, A. J. J. M. van Breemen, J. Shen, Q. Gao, M. G. Ivan, K. Reimann, E. R. Meinders, and G. H. Gelinck, "Multilevel Information Storage in Ferroelectric Polymer Memories," *Adv. Mater.*, vol. 23, no. 36, pp. 4146–4151, 2011.
- [38] R. Schroeder, L. A. Majewski, and M. Grell, "All-Organic Permanent Memory Transistor Using an Amorphous, Spin-Cast Ferroelectric-like Gate Insulator," *Adv. Mater.*, vol. 16, no. 7, pp. 633–636, 2004.
- [39] R. Schroeder, L. A. Majewski, M. Voigt, and M. Grell, "All-organic single-transistor permanent memory device," in *Symposium D Materials and Processes for Nonvolatile Memories*, 2004, vol. 830.
- [40] K. N. N. Unni, R. De Bettignies, S. Dabos-Seignon, and J. M. Nunzi, "A nonvolatile memory element based on a quaterthiophene field-effect transistor," *Mater. Lett.*, vol. 59, no. 10, pp. 1165–1168, 2005.
- [41] G. H. Gelinck, a. W. Marsman, F. J. Touwslager, S. Setayesh, D. M. De Leeuw, R. C. G. Naber, and P. W. M. Blom, "All-polymer ferroelectric transistors," *Appl. Phys. Lett.*, vol. 87, no. 9, pp. 23–25, 2005.
- [42] A. C. Nguyen and P. S. Lee, "Ferroelectric copolymer P (VDF-TrFE) as gate dielectric in organic field effect transistors for memory application devices," pp. 0–3, 2006.